EXPERIMENTAL OVERVIEW ON FLUCTUATIONS OF CONSERVED CHARGES*

Toshihiro Nonaka

Univsersity of Tsukuba, Japan

*Received 29 July 2022, accepted 20 September 2022,
published online 14 December 2022*

The phase diagram of the QCD matter can be explored in heavy-ion collisions by measuring event-by-event fluctuations of conserved charges. In these proceedings, we will introduce the known issues for measurements of higher-order fluctuations, and discuss how we have overcome them. We will then report on some of the recent experimental results and their interpretations. Finally, the future prospects of the fluctuation measurements will be discussed.

DOI:10.5506/APhysPolBSupp.16.1-A14

1. Introduction

One of the ultimate goals of heavy-ion collision (HIC) experiments is to understand the phase structure of Quantum Chromo-Dynamics (QCD) charactrized by temperature, T, and baryon chemical potential, μ_B. The phase transition from the Quark–Gluon Plasma (QGP) to the hadronic gas at $\mu_B = 0$ MeV was shown by the lattice QCD (LQCD) calculation [1] to be a smooth crossover, while there is no direct experimental evidence for the crossover. Various model calculations claim that the 1$^{\mathrm{st}}$-order phase transition appears at finite μ_B region, leading to the existence of the QCD critical point.

The QCD phase structure can be investigated in HIC through the measurements of event-by-event fluctuations of conserved charges such as net-charge, net-baryon, and net-strangeness number [2–4]. The fluctuations represent the shape of the distribution, which can be characterized by r^{th}-order cumulant: $C_r = \mu_r - \sum_{m=1}^{r-1} \binom{r-1}{m-1} C_m \mu_{r-m}$, with μ_r being the r^{th}-order non-central moment. Higher-order cumulants are predicted to be more sensitive to the phase structure. Experimentally, however, the net-particle number distributions are modified by various experimental artifacts and,

* Presented at the 29$^{\mathrm{th}}$ International Conference on Ultrarelativistic Nucleus–Nucleus Collisions: Quark Matter 2022, Kraków, Poland, 4–10 April, 2022.

therefore, the measured cumulants are different from the true ones for the generated distributions. Hence, lots of analysis techniques have been developed to extract the true signal. After considering all possible effects, some experimental results seem to exhibit hints about the QCD phase structure.

This contribution is organized as follows. In Sec. 2, some of the important effects and correction approaches for higher-order fluctuation measurements will be reviewed. In Sec. 3, recent experimental results will be shown and their interpretations will be discussed. Finally, future prospects will be mentioned in Sec. 4.

2. Experimental challenges

2.1. Acceptance correction

The efficiency correction on cumulants depends on the distribution of the detector efficiency. The simplest scenario is that the efficiency follows the binomial distribution, where the correction formulas can be derived in a straightforward way [5–7]. There are other two general methods, unfolding approach [8] and the moment expansion [9], which can be applied to any efficiency distribution. The methods are demonstrated by STAR [10, 11] and HADES [12].

It is also important to consider the effect of the limited acceptance in transverse momentum p_{T}. The effect is studied in Ref. [13] in terms of the baryon-to-charge 2$^{\mathrm{nd}}$-order cumulant ratio by using the STAR data. In Fig. 1, the ratio is constructed from the STAR data with and without p_{T} acceptance correction, which results in different values and conclusions in temperature comparing to the lattice QCD calculations. This study indicates that one should perform p_{T} acceptance correction while comparing to the theoretical calculations integrated in p_{T}.

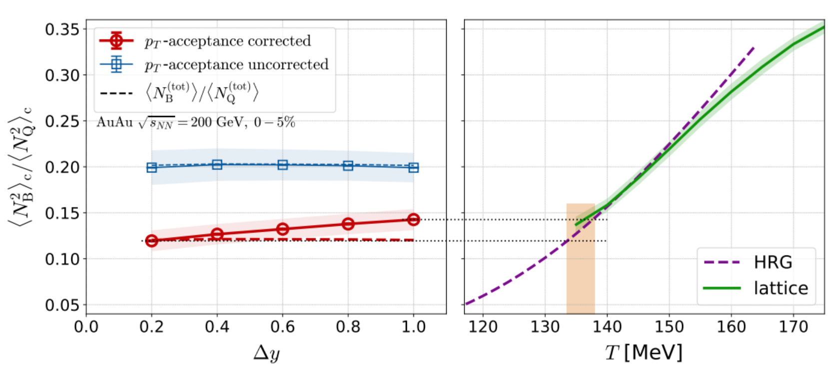

Fig. 1. Rapidity acceptance dependence of the 2$^{\mathrm{nd}}$-order baryon-to-charge cumulant ratio (left) reconstructed from STAR data for Au+Au most central collisions at 200 GeV (right) from the HRG and LQCD calculations [14].

2.2. Initial volume fluctuations

In HIC, the relation between initial geometry and the final-state observable is in not one-to-one corresponding, which is referred to as initial volume fluctuations (VF). It is known that the value of higher-order cumulants is modified due to VF, while the C_1 value is not affected by construction. One simple way to suppress the effect of VF is to apply the Centrality Bin Width Correction (CBWC) [15], although it cannot eliminate the VF depending on the centrality resolution in the measurements.

There is another correction approach proposed in Refs. [16, 17]. The method utilizes the initial volume cumulants determined by model calculations, and it is justified under the assumption of independent particle production (IPP) [18]. The method has been extended by including higher-order contribution of initial volume cumulants, where the IPP assumption is no longer required. The method is demonstrated by the HADES Collaboration [12].

2.3. Pileup correction

The event pileup is a random superposition among more than one single-collision events. The probability of the pileup events becomes much more significant in fixed-target experiments compared to the collider experiments. It was pointed out that the higher-order cumulants get artificially enhanced in central collisions by pileup events. To solve the issue, the pileup correction has been developed [19]. The method utilizes the true reference multiplicity distribution from single-collision events, which can be extracted in a data-driven way [20].

The pileup correction has been applied to the STAR data at fixed-target Au+Au collisions at $\sqrt{s_{NN}} = 3$ GeV [21]. The reference multiplicity distribution for single-collision events is extracted by using the unfolding approach, which yields 0.46% fraction of pileup collisions in minimum bias events.

3. Experimental results

3.1. Deuteron number fluctuations

According to the model calculations, deuteron number fluctuations and their correlation with protons are sensitive to the production mechanism of deuterons [22]. The top panel in Fig. 2 shows collision energy dependence of cumulant ratios up to the 4^{th}-order of deuteron number distribution and the 2^{nd}-order proton–deuteron correlations in Au+Au collisions measured by the STAR Collaboration. It is found that the collision energy dependence is qualitatively reproduced by UrQMD+coalescence model calculations, while the Canonical Ensemble (CE) calculations can also describe the overall trend of the results. The proton–deuteron correlations show negative values for all collision energies, which rules out a coalescence model with correlated production of protons and neutrons.

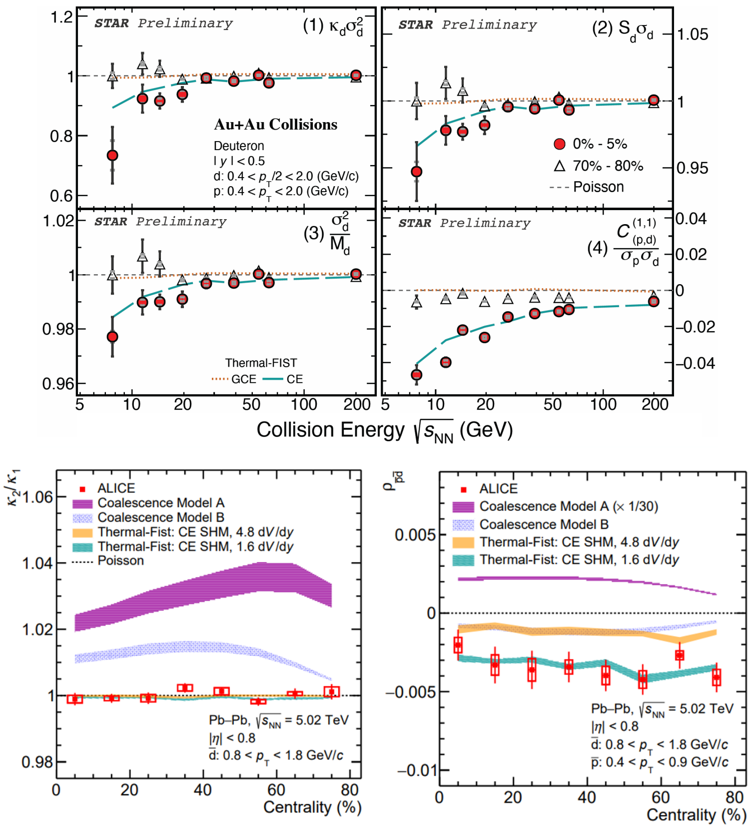

Fig. 2. (Top) Deuteron number fluctuations and proton–deuteron correlations as a function of collision energy in Au+Au collisions. (Down) Antideuteron number fluctuations and correlations between antiprotons and antideuterons as a function of collision centrality in Pb+Pb 5.02 TeV collisions.

The two down panels in Fig. 2 show the centrality dependence of the 2$^{\text{nd}}$-order cumulant ratio of antideuteron number distribution and the correlation between antideuterons and antiprotons measured by the ALICE Collaboration for Pb+Pb 5.02 TeV collisions [23]. The cumulant ratio is consistent with the Poisson expectation and CE calculations. The antideuterons and antiprotons correlations show negative values for all centralities, which is consistent with CE calculations having a smaller correlation volume than that from net-proton fluctuations.

3.2. Net-proton fluctuations

The collision energy dependence of net-proton C_4/C_2 has been measured by the STAR Collaboration [11, 24]. In Fig. 3, the ratio of the 70–80% peripheral collisions is flat with respect to the collision energy, while the ratio of the 0–5% most central collisions shows nonmonotonic collision energy dependence having the minimum and enhancement at 19.6 GeV and 7.7 GeV, respectively. It was found that the collision energy dependence has the nonmonotonicity with 3.1σ level in the most central collisions, which could be a signal from the critical point.

Results from the fixed-target experiment at the HADES and STAR experiments are also shown in Fig. 3 for 2.4 and 3.0 GeV Au+Au central collisions, respectively. Both the results are consistent within uncertainties, where the strong enhancement observed in 7.7 GeV no longer exists. More importantly, the result at 3 GeV can be reproduced by UrQMD calculations in which the hadronic interactions and baryon number conservation are dominated. Hence, these data imply that the QCD critical region could only exist at the collision energy above 3 GeV.

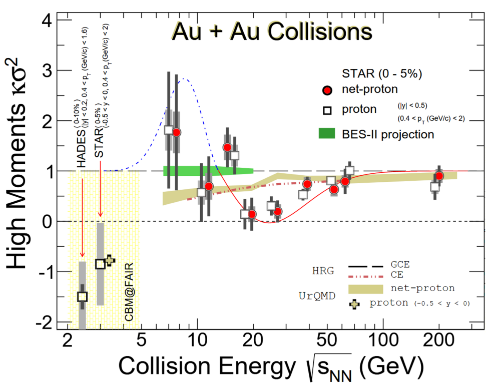

Fig. 3. Collision energy dependence of net-proton C_4/C_2.

Figure 4 shows the charged particle multiplicity dependence of higher-order cumulant ratios up to the 6$^{\text{th}}$-order of the net-proton distributions for p+p, Ru+Ru, Zr+Zr, and Au+Au collisions at 200 GeV. All ratios are found to decrease with increasing the charged particle multiplicity, and smoothly connect among different collision systems. Most importantly, the 5$^{\text{th}}$- and 6$^{\text{th}}$-order ratios go negative with increasing the multiplicity, and approach the values from LQCD calculations [25]. Therefore, the results indicate that the created system approaches the thermalized medium at the high multiplicity region.

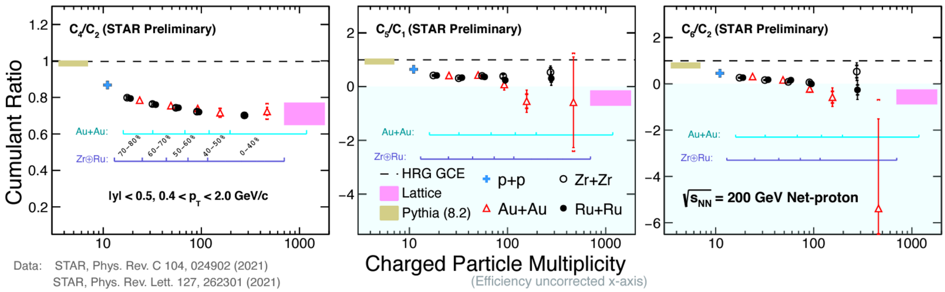

Fig. 4. Charged particle multiplicity dependence of net-proton C_4/C_2, C_5/C_1, and C_6/C_2 for p+p, Ru+Ru, Zr+Zr, and Au+Au collisions at 200 GeV.

4. Future prospects

4.1. Hyperon number fluctuations

The hyperon number fluctuation is of interest since it carries both baryon and strangeness, which is important especially for baryon–strangeness correlations [26]. The correlations among conserved charges are predicted by the LQCD calculations to be sensitive not only to the temperature of the created system but also to the magnetic field created in noncentral HIC [27, 28].

Experimentally, hyperons are reconstructed together with combinatorial backgrounds through the invariant mass technique, and it is not possible to identify the signal and background particles on a track-by-track basis. This fact forces us to apply very tight topological cuts for hyperon reconstructions, leading to lower reconstruction efficiencies and larger statistical uncertainties on hyperon number fluctuations. To solve the issue, a new method called purity correction has been proposed [29]. The effect of the combinatorial backgrounds can be subtracted from the measurements by using sideband cumulants. The method enables us to achieve the best statistical significance of the hyperon number fluctuations.

4.2. Crossover and critical point search

The STAR Collaboration plans to collect up to around 18 billion minimum bias event statistics in Au+Au 200 GeV collisions from 2023 to 2025 at RHIC [30]. It corresponds to 18 times larger statistics than the published data [25]. The ALICE Collaboration also plans precise measurements of net-proton 6^{th}-order fluctuations at the LHC Run 3 [31]. These measurements will enable us to extract definitive physics messages on a smooth crossover at small μ_B region.

The STAR Collaboration completed the phase 2 program of the BES focusing on the collision energy of $7 < \sqrt{s_{NN}} < 20$ GeV to collect 10–20 times larger event statistics compared to BES-I. The strong enhancement of net-proton 4$^{\rm th}$-order fluctuation observed at $\sqrt{s_{NN}} \approx 7.7$ GeV will be examined with the better precision. It will be also important to confirm the peak structure predicted by theoretical model calculations around the critical point [3]. As shown by the dotted line in Fig. 3, the predicted peak is likely to exist from 3 GeV to 7.7 GeV. This scenario will be precisely tested by future experiments, *e.g.*, the CBM experiment at FAIR, the MPD experiment at NICA, the CEE experiment at HIAF, and the JPARC-HI

REFERENCES

[1] Y. Aoki *et al.*, *Nature* **443**, 675 (2006).

[2] M.A. Stephanov, K. Rajagopal, E.V. Shuryak, *Phys. Rev. D* **60**, 114028 (1999).

[3] M. Stephanov, *Phys. Rev. Lett.* **107**, 052301 (2011).

[4] A. Majumder, B. Müller, *Phys. Rev. C* **74**, 054901 (2006).

[5] A. Bzdak, V. Koch, *Phys. Rev. C* **86**, 044904 (2012).

[6] M. Kitazawa, M. Asakawa, *Phys. Rev. C* **86**, 024904 (2012); *Erratum ibid.* **86**, 069902 (2012).

[7] T. Nonaka *et al.*, *Phys. Rev. C* **95**, 064912 (2017).

[8] S. Esumi *et al.*, *Nucl. Instrum. Methods Phys. Res. A* **987**, 164802 (2021).

[9] T. Nonaka *et al.*, *Nucl. Instrum. Methods Phys. Res. A* **906**, 10 (2018).

[10] STAR Collaboration (J. Adam *et al.*), *Phys. Rev. Lett.* **126**, 092301 (2021).

[11] STAR Collaboration (M.S. Abdallah *et al.*), *Phys. Rev. C* **104**, 024902 (2021).

[12] HADES Collaboration (J. Adamczewski-Musch *et al.*), *Phys. Rev. C* **102**, 024914 (2020).

[13] M. Kitazawa, S. Esumi, T. Nonaka, `arXiv:2205.10030 [hep-ph]`.

[14] D. Bollweg *et al.*, *Phys. Rev. D* **104**, 074512 (2021).

[15] X. Luo *et al.*, *J. Phys. G: Nucl. Part. Phys.* **40**, 105104 (2013).

[16] V. Skokov *et al.*, *Phys. Rev. C* **88**, 034911 (2013).

[17] P. Braun-Munzinger *et al.*, *Nucl. Phys. A* **960**, 114 (2017).

[18] T. Sugiura *et al.*, *Phys. Rev. C* **100**, 044904 (2019).

[19] T. Nonaka *et al.*, *Nucl. Instrum. Methods Phys. Res. A* **984**, 164632 (2020).

[20] Y. Zhang, Y. Huang, T. Nonaka, X. Luo, *Nucl. Instrum. Methods Phys. Res. A* **1026**, 166246 (2022).

[21] STAR Collaboration (M.S. Abdallah *et al.*), *Phys. Rev. Lett.* **128**, 202303 (2022).

[22] Z. Fecková, J. Steinheimer, B. Tomášik, M. Bleicher, *Phys. Rev. C* **93**, 054906 (2016).

[23] ALICE Collaboration, `arXiv:2204.10166 [nucl-ex]`.

[24] STAR Collaboration (J. Adam *et al.*), *Phys. Rev. Lett.* **126**, 092301 (2021).
[25] STAR Collaboration (M.S. Abdallah *et al.*), arXiv:2105.14698 [nucl-ex].
[26] Z. Yang, X. Luo, B. Mohanty, *Phys. Rev. C* **95**, 014914 (2017).
[27] V. Koch, A. Majumder, J. Randrup, *Phys. Rev. Lett.* **95**, 182301 (2005).
[28] H.T. Ding, S.T. Li, Q. Shi, X.D. Wang, *Eur. Phys. J. A* **57**, 202 (2021).
[29] T. Nonaka, *Nucl. Instrum. Methods Phys. Res. A* **1039**, 167171 (2022).
[30] The STAR Beam Use Request for Run-22 and data taking in 2023–25, https://drupal.star.bnl.gov/STAR/starnotes/public/sn0773
[31] Z. Citron *et al.*, *CERN Yellow Rep. Monogr.* **7**, 1159 (2019).